Hindawi
Advances in Materials Science and Engineering
Volume 2020, Article ID 2074232, 15 pages
https://doi.org/10.1155/2020/2074232

Research Article

Effect of Nanoclays on Moisture Susceptibility of SBS-Modified Asphalt Binder

Han Wang, Yinchuan Guo, Aiqin Shen, Xiaolong Yang, and Peng Li

School of Highway, Chang'an University, Xi'an 710064, Shaanxi, China

Correspondence should be addressed to Han Wang; 876681215@qq.com and Yinchuan Guo; silver007007@163.com

Received 8 November 2019; Revised 12 January 2020; Accepted 1 February 2020; Published 26 February 2020

Academic Editor: Marinos Pitsikalis

Moisture susceptibility plays an important role in the damage of asphalt pavement. Failure occurs when asphalt is removed from the aggregate particles due to the decreased adhesion between the asphalt and aggregate in comparison with that between water and the aggregate. In recent years, efforts utilizing nanomaterials to improve the diverse properties of asphalt have proven to be effective. In this study, three types of nanoclays were used to modify styrene-butadiene-styrene- (SBS-) modified asphalt. The resistances to water damage of the modified binders were evaluated using the surface free energy (SFE) and atomic force microscopy (AFM). The results revealed that the total SFE decreased and the energy ratio (ER) increased when the asphalt binder was modified with the nanoclays, indicating that the addition of nanoclays can improve the moisture resistance of these aggregate-binder systems. After immersion, a decreased amount of bee structures was observed in both the SBS and nanoclay-modified asphalts due to the interactions between water and bitumen. However, the residual amount of bee structures was higher in the nanoclay-modified asphalts than in the SBS-modified asphalt, indicating that the addition of nanoclay makes the surface morphology of asphalt more resistant to water damage. Finally, freeze-thaw splitting tests were used to verify the results obtained through the SFE and AFM tests.

1. Introduction

Asphalt pavement is incessantly subjected to the combination of repeated vehicle loading and complex environmental loading throughout its years of service, resulting in cracking, rutting, and water damage to the asphalt surface [1,2]. These forms of wear degrade the performance and reduce the service life of asphalt pavement, resulting in considerable economic losses [3].

Moisture damage plays an important role in the damage of the asphalt pavement. Failure may occur when asphalt is removed from aggregate particles due to the worsened adhesion between the asphalt and aggregate compared to that between water and the aggregate [4, 5]. The abovementioned phenomenon may result from the existence of several pathways through which moisture may permeate into the internal structure of the pavement. For instance, moisture may enter the pavement through cracks, voids, road shoulder edges, or through the bottom of the asphalt pavement by capillary action [6].

To avoid or slow the process of water damage, a widely adopted measure is the modification of the asphalt or aggregates using various materials as modifiers to improve the performance of the asphalt mixture [7, 8]. The impact of using lime to modify asphalt was found to be capable of improving the moisture resistance of hot mix asphalt (HMA) mixtures [9]. The laboratory results of porous asphalt mixtures obtained by Jiao et al. showed that the use of crumb rubber (CR) and tafpack super (TPS) could improve the resistance of styrene-butadiene-styrene- (SBS-) modified asphalt towards water damage [10].

In recent years, with the development of nanotechnology, attempts using nanotechnology to enhance the performances of asphalt and asphalt mixtures have become a common research trend [11–15]. Several studies have been conducted that aim to reduce the moisture damage of asphalt and asphalt mixtures. Mamun and Arifuzzaman added a certain amount of carbon nanotubes (CNTs) to styrene-butadiene (SB) and styrene-butadiene-styrene (SBS) and

found that the CNT-polymer-modified asphalt showed better resistance towards moisture damage than the corresponding polymer-modified asphalt [7]. The research of Das and Singh suggested that the contribution of the nanosized hydrated lime (NHL) filler was more significant than that of the regular-sized hydrated lime (RHL) filler in improving the bond strength and moisture resistance of asphalt mastic [16]. Additionally, it was revealed by Sezavar et al. through a group method of data handling (GMDH) algorithm that nanosilica could improve the moisture stability of asphalt mixtures [17].

Over the last few years, there has been a growing interest in the use of nanoclays to improve the water resistance of asphalt. Goh et al. found that adding nanoclays to asphalt could significantly reduce the potential for water damage of the mixture [18]. Similarly, Omar et al. [5] and Ashish et al. [19] also demonstrated that using nanoclays as modifiers is beneficial to the moisture resistance of asphalt. Although the majority of researchers confirmed that nanoclay has the potential to reduce moisture damage to asphalt, there are still researchers who hold different views. In the research of Lopez-Montero et al. [20], a nanoclay-modified mixture exhibited similar behaviors to that of the control mixture when fresh mixtures were subjected to moisture damage. Moreover, Hossain et al. [21] evaluated the resistance to moisture damage of binders modified with different dosages of two nanoclays. They suggested that unless these binders were modified with an antistripping agent or other additives, the nanoclay-modified binders would have poorer moisture resistances than the base binder.

One of the nanoclays that is currently widely used is montmorillonite (MMT) [22]. Due to the small size of MMT and the existence of a large number of exchangeable cations in its interlayers, bitumen molecules can easily intercalate into the interlayers of MMT by reacting with the exchangeable cations [23, 24]. Additionally, MMT can be transformed into organic montmorillonite (OMMT) through organic modification. After modification, the spacing between the layers of OMMT increases, making it easier for asphalt molecules to intercalate [25]. Another potential nanoclay is calcined-layered double hydrotalcite (LDH). LDH is composed of octahedral brucite layers and exchangeable interlayer anions [26]. Due to its large surface area, high anion-exchange capacities, and flexible interlayer space, it functions well in intercalating anionic compounds [27]. Furthermore, both LDH and MMT possess advantages, such as their widespread existence in nature, low-cost, and mature production processes [25, 28].

Traditional methods used for studying moisture damage include the boiling, immersion Marshall, and freeze-thaw splitting tests, among others [5]. Although many studies have been performed using these traditional methods, there are still some deficiencies. A large number of studies have demonstrated that the water damage of an asphalt binder system occurs at the molecular scale, or possibly even at the nanoscale [29–32]. However, the traditional evaluation methods mentioned above cannot reveal the processes and mechanisms of water damage at the molecular or nanoscales.

In addition, it is worth mentioning that although the traditional methods have some limitations, they can be used to verify the results obtained from other tests [5]. Amongst the methods developed more recently are surface free energy (SFE) [19, 33] and atomic force microscopy (AFM) [34, 35].

The SFE method is a method used to quantitatively examine the moisture damage of asphalt from the perspective of thermodynamic changes [36]. The SFE method has been confirmed to possess great potential in predicting moisture damage [5, 19, 37]. Using this method, Ashish et al. [19] and Omar et al. [5] evaluated the moisture susceptibility of asphalt and concluded that the addition of nanoclays could improve this property of the asphalt. However, the opposite conclusion was reached by Hossain et al. using the same method [21].

Additionally, AFM is a method used to study the performance of an asphalt binder at the microscale [25, 38, 39]. Recently, it has been widely used due to its provision of three-dimensional imaging, as well as its ability to evaluate roughness and adhesion [34, 40]. The interactions between the AFM tip and asphalt can be used to simulate the bonds between the aggregates and asphalt binders [34]. Liu et al. used AFM technology to measure the adhesion of four types of bitumen under dry and wet conditions, proving that SBS-modified bitumen has better resistance to water damage than the other three types of tested bitumen [31]. Using the same method, dos Santos et al. soaked asphalt samples in water and observed the changes in their surface micromorphologies for different soaking times [41]. Nevertheless, most studies concerning the moisture susceptibility of nanoclay-modified asphalt binders have not focused on the changes in the microstructures of these binders after immersion.

Therefore, to further study the impact of nanoclays on the moisture resistance of asphalt binders, three types of nanoclays, i.e., organic montmorillonite A, organic montmorillonite B, and calcined-layered double hydrotalcite, were selected to prepare nine types of nanoclay-modified asphalts using different dosages. The moisture resistances of these binders were evaluated using the SFE approach. Then, the two asphalts with the great resistances to water damage as determined by the SFE tests, as well as the control asphalt, were selected for AFM examination. The prepared AFM samples were divided into an immersion group and a nonimmersion group. The nanomorphologies of the samples in both the immersion and nonimmersion groups were observed to determine the effects of water on the microstructures of the asphalt binders. The effects of the nanoclays on the resistance of asphalt to water damage were also examined. Finally, freeze-thaw splitting tests were used to verify the results obtained through SFE and AFM.

2. Materials and Methods

2.1. Materials

2.1.1. Asphalt. SBS-modified asphalt, obtained from Gansu Road & Bridge Construction Group Co., Ltd., was used as the matrix asphalt and control group in this study. The SBS-

modified asphalt was prepared using SK-90# base asphalt with a 5% SBS modifier. The technical properties of the asphalt are presented in Section 2.2 together with the properties of the nanoclay-modified asphalt.

Three types of nanoclays, i.e., organic montmorillonite A (OMMT A), organic montmorillonite B (OMMT B), and calcined-layered double hydrotalcite, were used in this study for the modification of asphalt. The specific components of these nanoclays are presented in Table 1, and the microstructures of the three nanoclays are illustrated in Figures 1(a) and 1(c), respectively.

2.1.2. Aggregates. The type of aggregate used to fabricate the asphalt mixture for the freeze-thaw splitting tests was basalt. The physical properties of basalt were measured according to the Technical Specifications for Construction of Highway Asphalt Pavements (JTGF40-2004) of China. The main physical properties of the aggregate are presented in Tables 2–4.

2.2. Preparation of Modified Asphalt. The modified bitumen samples were prepared by adding three different percentages of each nanoclay (1, 3, and 5% by weight of the bitumen) into the binder. The reason for not using a greater amount of these additives is that too much clay would reduce the performance of the asphalt at low temperatures [25] (see, for example, the ductility of the asphalt under a low-temperature condition listed in Table 5). 500 ± 20 grams of the asphalt binder was poured into containers and heated at 175°C for 1 h before the modification process. To achieve this heating, the asphalt containers were placed in an oven.

The nanoclays were heated at 80°C for 1.5 h to remove moisture before they were added into the binder. After heating, the nanoclays were steadily added to the asphalt binder. They were first mixed at 1,000 revolutions per minute (RPM) for 15 min, followed by 5,000°RPM for 1 h to ensure that all additive particles were uniformly dispersed in the asphalt. The shear rate was then decreased to 1,000°RPM and the mixing process was continued for another 15 min to eliminate the bubbles generated by the high-speed shear. All mixing steps were performed using a high-shear mixer.

The basic performances of the SBS-modified asphalt and nanoclay-modified asphalts were determined through the penetration, softening point, and ductility tests according to the Technical Specifications for Construction of Highway Engineer (JTGF 40-2004) of China. The results of these tests are presented in Table 5.

In this table, "OMMT A-1" indicates the asphalt modified with 1% OMMT A by weight of the bitumen, and so on.

2.3. Preparation of Asphalt Mixtures. Asphalt mixture samples for the freeze-thaw splitting tests were prepared according to the Standard Test Method of Bitumen and Bituminous Mixtures for Highway Engineering (JTGE20-2011) and the Technical Specifications for Construction of Highway Asphalt Pavements (JTGF40-2004) of China.

The gradation of the aggregates in this study is AC-13 for the dense asphalt mixtures, and the passing rates of the aggregates are presented in Table 6.

The optimum asphalt ratio was determined by the Marshall mixture design method. The asphalt mixture was prepared at 180°C. For the SBS-modified asphalt, which was used as the matrix bitumen, the optimum asphalt ratio was determined to be 6.2% of the total mass of the coarse aggregate, fine aggregate, and filler. The nanoclay was added through a dry process. The same weight of the powder filler was replaced by the nanoclay. Additionally, because the mixture was prepared for the freeze-thaw splitting test, the Marshall samples only needed to be compacted 50 times on both sides instead of 75 times, according to the JTGE20-2011 of China.

2.4. Surface Free Energy (SFE) Tests. The surface free energy (SFE) is defined as the magnitude of energy needed to create a unit of surface area in a vacuum [42]. It may be considered as a useful method for evaluating the effect of water on the strength of an asphalt mixture [5,36].

The surface energy consists of several force components that exist between molecules, which are mainly an acidic component, basic component, and Lifshitz–van der Waals component [33]. Equation (1) can be used to describe the relationship between the surface energy and these force components that exist between molecules:

$$\gamma = \gamma^{\mathrm{lw}} + \gamma^{\mathrm{p}} = \gamma^{\mathrm{lw}} + 2\sqrt{\gamma^{+}\gamma^{-}}. \quad (1)$$

In this equation, γ represents the total surface free energy, γ^{lw} represents the Lifshitz–van der Waals component, γ^{p} represents the polarity component, γ^{+} represents the Lewis acid component (erg/cm^2), and γ^{-} represents the Lewis base component (erg/cm^2).

The contact angle is an index that can be used to calculate the SFE. To measure the contact angle, bitumen samples with smooth surfaces are required. To achieve this, 3-4 g of asphalt in a fluid state was dripped onto a glass slide. Then, the glass slide was placed horizontally on a base plate. An electric stove under the base plate was used to heat the asphalt. The asphalt was heated such that it flowed freely and formed a smooth surface. To minimize the aging of the asphalt, the temperature of this process was maintained at 175°C for 1 min. After undergoing the abovementioned steps, the samples with smooth surfaces were then cooled at room temperature and left for one day before measuring the contact angle.

Several types of liquids with known SFE components were selected as probe liquids for measuring the surface-free energy of the asphalt binders on the basis of previous studies [43–45]. The SFE components of these probe liquids are presented in Table 7 [46].

To obtain accurate contact angles, each probe liquid was dropped at five positions that were uniformly distributed on the smooth surface of a sample. The contact angle testing was performed using a Contact Angle System OCA 20 from the Germany Dataphysics company, as described in a previous study [47].

Table 1: Specific compositions of the nanoclays.

Sample	OMMT A	OMMT B	LDH
SiO_2 (%)	71.35	72.21	1.05
Al_2O_3 (%)	18.53	19.16	98.61
MgO (%)	3.05	3.11	—
Fe_2O_3 (%)	2.77	2.22	0.02
K_2O (%)	1.30	0.78	0.02
CaO (%)	1.20	0.25	0.02
SO_3 (%)	0.47	0.98	—
Cl (%)	0.41	0.60	—
Na_2O (%)	0.32	0.23	0.23
TiO_2 (%)	0.28	0.20	—
P_2O_5 (%)	0.24	0.19	—
MnO (%)	0.03	0.04	—
ZrO_2 (%)	0.01	0.01	—
ZnO (%)	0.01	0.01	—
SrO (%)	0.01	0.00	—
Rb_2O (%)	0.00	0.00	—
Ga_2O_3 (%)	—	—	0.05
Total (%)	100.00	100.00	100.00
LOI	28.70	32.79	33.93

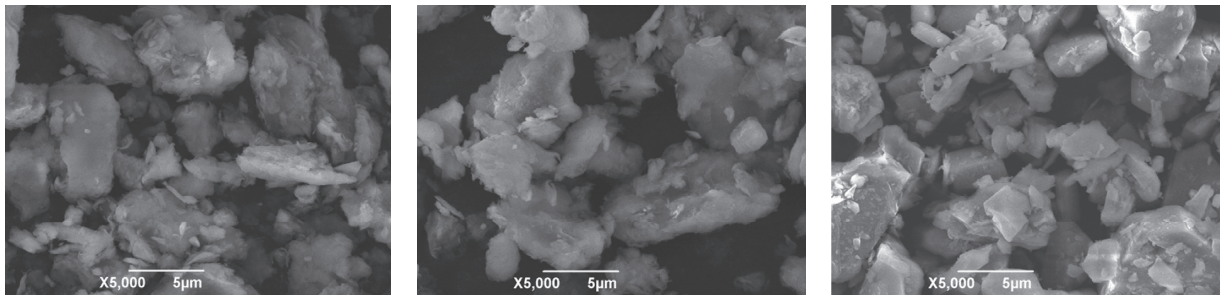

(a) (b) (c)

Figure 1: Microstructures of the nanoclays: (a) OMMT A, (b) OMMT B, and (c) LDH.

Table 2: Physical properties of the coarse aggregate.

Property	Standard	Specification limit	Result
Apparent specific gravity (g/cm^3)	JFGF 40-2004	≥2.60	2.92
Bulk specific gravity (g/cm^3)	JFGF 40-2004	—	2.87
Water absorption (%)	JFGF 40-2004	≤2.0	0.54
Content of soft rock (%)	JFGF 40-2004	≤3	1.80
Crushed stone value (%)	JFGF 40-2004	≤26	21.00
Firmness (%)	JFGF 40-2004	≤12	5.60
Water washing method < 0.075 mm particle content (%)	JFGF 40-2004	≤1	0.65
Abrasion value (%)	JFGF 40-2004	≤28	23.25

The average values of the contact angles obtained from the parallel experiments were then substituted into equation (2) to determine the SFE components of the asphalt:

$$(1 + \cos\Phi)\gamma_{pl} = 2\sqrt{\gamma_b^{lw}\gamma_{pl}^{lw}} + 2\sqrt{\gamma_b^{+}\gamma_{pl}^{-}} + 2\sqrt{\gamma_b^{-}\gamma_{pl}^{+}}. \quad (2)$$

In this equation, Φ represents the measured contact angle; γ_{pl} represents the total SFE of the probe liquids (erg/cm^2); γ_b^{lw} and γ_{pl}^{lw} represent the Lifshitz–van der Waals components of the bitumen and probe liquids (erg/cm^2), respectively; γ_b^{+} and γ_{pl}^{+} represent the acidic components of the bitumen and probe liquids (erg/cm^2), respectively; and γ_{pl}^{-} and γ_b^{-} represent the basic components of the probe liquids and bitumen (erg/cm^2), respectively.

Past studies have found that the bond between the asphalt and aggregate is weaker than that between water and the aggregate, which is a primary cause of water damage [5]. To study the moisture damage from the perspective of thermodynamic changes, two indices were applied. The first is the work of debonding, which is described as the energy

Table 3: Physical properties of the fine aggregate.

Property	Standard	Specification limit	Result
Apparent specific gravity (g/cm^3)	JFGF 40-2004	≥2.5	2.751
Bulk specific gravity (g/cm^3)	JFGF 40-2004	—	2.599
Sand equivalent (%)	JFGF 40-2004	≥60	70
Methylene blue value (g/kg)	JFGF 40-2004	≤2.5	1.3
Angularity (fluidity) (s)	JFGF 40-2004	≥30	39

Table 4: Physical properties of the filler.

Property	Standard	Specification limit	Result
Apparent density (t/m^3)	JFGF 40-2004	≥2.5	2.727
Hydrophilic coefficient	JFGF 40-2004	<0.8	0.6
Plasticity index (%)	JFGF 40-2004	<4	2
Water content (%)	JFGF 40-2004	≤1	0.2
Appearance	JFGF 40-2004	No clumps	No clumps

Table 5: Basic performances of the asphalts.

Asphalt type	Penetration (25°C, 100 g, 5 s) (0.1 mm)	Softening point (°C)	Ductility (5°C, 5 cm/min) (cm)
Control asphalt	57.7	89.3	39.2
OMMT A-1	54.4	91.5	37.8
OMMT A-3	51.5	94.8	31.2
OMMT A-5	52.6	94.5	33.5
OMMT B-1	55.2	93.1	30.7
OMMT B-3	52.7	94.7	26
OMMT B-5	48.6	80.1	22.3
LDH-1	55.4	89.5	34
LDH-3	55.8	90.3	37.3
LDH-5	56.9	82	35.2

Table 6: Gradation of the aggregates.

Sieve size (mm)	16	13.2	9.5	4.75	2.36	1.18	0.6	0.3	0.15	0.075
Lower-upper limits	100	90–100	68–85	38–68	24–50	15–38	10–28	7–20	5–15	4–8
Passing percent (%)	100	95	76.5	53	37	26.5	19	13.5	10	6

Table 7: SFE components of the probe liquids.

Liquid	γ	$\gamma+$	$\gamma-$	γ^{lw}
Water	72.8	25.5	25.5	21.6
Glycerol	63	3.6	57.4	34
Formamide	58	2.28	39.6	39

reduction of the asphalt-aggregate system with the displacement of the asphalt binder from the asphalt-aggregate interface. The other is the energy ratio (ER).

To calculate these two indices, the SFE components of the aggregates are required. In this paper, the SFE components of the aggregates, i.e., limestone1, limestone2, and basalt, were obtained from previous studies by Hossain et al. [21] and Qazizadeh et al. [46]. The SFE components of these aggregates are shown in Table 8.

Equations (3) and (4) could be, respectively, used to calculate the work of adhesion in dry conditions and debonding in the presence of water:

$$W_{ab} = 2\sqrt{\gamma_b^{lw}\gamma_a^{lw}} + 2\sqrt{\gamma_a^{+}\gamma_b^{-}} + 2\sqrt{\gamma_a^{-}\gamma_b^{+}}. \quad (3)$$

In this equation, W_{ab} represents the work of adhesion in dry conditions; γ_b^{lw} and γ_a^{lw} represent the Lifshitz–van der Waals components of the bitumen and aggregates (erg/cm^2), respectively; γ_a^{+} and γ_b^{+} represent the acid components of the aggregates and bitumen (erg/cm^2), respectively; and γ_b^{-} and γ_a^{-} represent the base components of bitumen and aggregates (erg/cm^2), respectively.

$$W_{abw} = \gamma_{aw} + \gamma_{bw} + \gamma_{ab}. \quad (4)$$

In this equation, W_{abw} represents the work of debonding in the presence of water. γ_{aw}, γ_{bw}, and γ_{ab} represent the surface energies of the aggregate-water interface, bitumen-water interface, and aggregate-bitumen interface, respectively. The possibility of replacing asphalt with water in the

Table 8: SFE components of the aggregates.

Aggregates	γ	$\gamma+$	$\gamma-$	γ^{lw}
Limestone1	219.9	13.0	540.7	51.9
Limestone2	222.18	11.81	561.47	59.32
Basalt	72.3	0.6	164	52.3

asphalt-aggregate system substantially depends on the surface energy [5].

The energy ratio (ER), which quantifies the moisture damage potential, can be calculated using equation (5). A high ER value indicates that the asphalt mixture has considerable resistance to moisture damage [43]:

$$\mathrm{ER} = \left|\frac{W_{ab}}{W_{abw}}\right|. \quad (5)$$

In this equation, W_{ab} represents the work of adhesion under dry conditions and W_{abw} represents work of debonding in the presence of water.

2.5. Atomic Force Microscopy. Atomic force microscopy is an excellent means of studying the surface microstructures of asphalt. It has been widely used in recent years due to its provision of three-dimensional imaging, as well as its capabilities of evaluating roughness and adhesion [34, 40, 48].

To prepare the AFM test samples, hot liquid bitumen, which was heated in advance to 170°C, was placed on a rectangular region of a clean glass slide. Then, the microscope glass slide containing bitumen was placed in an oven for 2 min. The oven temperature was set at 170°C to allow the asphalt binder to spread. After the abovementioned steps, the glass slide was taken out from the oven and cooled at room temperature for one day.

The samples were then divided into an immersion group and a nonimmersion group to observe the changes of the micromorphologies of the asphalt samples after immersion in water. Both nanoclays modified- and SBS-modified asphalts were observed. The samples in the immersion group were soaked in water at 25°C for 24 h and then dried at 25°C for 72 h; samples in the nonimmersion group were sealed at 25°C before the AFM test.

The morphologies and relevant properties of the samples were tested using an Innova atomic force microscope with an OTESPA-R3 probe in the tapping mode. The nominal spring constant of the probe was 26 N/m, scanning frequency was 0.9°Hz, scanning range was 30 μm × 30 μm, and resolution was 512 × 512. All experiments were conducted using the same AFM probe.

2.6. Freeze-Thaw Splitting Test. The freeze-thaw splitting test is a traditional method used to evaluate the water sensitivity of asphalt mixtures. According to the Standard Test Methods of Bitumen and Bituminous Mixtures for Highway Engineering (JTGE 20-2011) of China, the indirect tensile strengths (ITS) of the Marshall specimens with and without undergoing the freeze-thaw process were measured. The sizes of these Marshall specimens were all Φ = 101.6 mm × 63.5 ± 1.3 mm.

The freeze-thaw process mentioned above includes 16 h of freezing at −18°C and 24 h of bathing in water at 60°C. Additionally, the Marshall specimens must undergo vacuum saturation before undergoing the freeze-thaw process.

After the indirect tensile strength was measured, the tensile strength ratio (TSR) of the samples was calculated using the following equation:

$$\mathrm{TSR} = \left|\frac{\mathrm{ITS1}}{\mathrm{ITS2}}\right|. \quad (6)$$

In this equation, ITS_1 represents the ITS of the samples that underwent the freeze-thaw process, while ITS_2 represents the ITS of the samples that did not undergo the freeze-thaw process.

2.7. Flowchart of Experimental Design. The flowchart for this study is shown in Figure 2.

3. Results and Discussion

3.1. SFE Test

3.1.1. Contact Angles of the Asphalt. The average contact angles of the asphalt samples are presented in Figure 3. In this figure, it can be observed that the contact angles varied between the asphalt binders when specific probe liquids were used. This variation resulted from the addition of nanoclays and reflected the change of the SFE components of the asphalt binder after modification.

To verify the validity of the experimental data of the contact angle, the $\gamma \cos \Phi$ and γ values of the different probe liquids were fitted linearly, as performed by Li et al. and Wang et al. [49,50]. The results are shown in Figure 4. The coefficient of linear fitting (R^2) is between 0.9887 and 1, which indicates a good linear relationship between γ and $\gamma \cos\Phi$. Therefore, the experimental data is valid.

As mentioned above, the contact angle may be used to calculate the SFE components of the asphalt, and these indices will be discussed next.

3.1.2. SFE Components of the Asphalt. Figures 5(a) and 5(b) show the SFE components of the modified asphalt binders. As the three types of nanoclays all have an abundance of positive and negative charges, general improvement can be clearly observed in the acidic and basic components of all modified binders, with exception of OMMT B-5. However, an inverse trend was observed for the values of the total SFE, also with an exception of OMMT B-5. The main reason for this decrease in the total SFE is that the addition of the nanoclays weakened the nonpolar components of the asphalt, which play a dominant role in the total SFE of the asphalt [5, 21]. The most

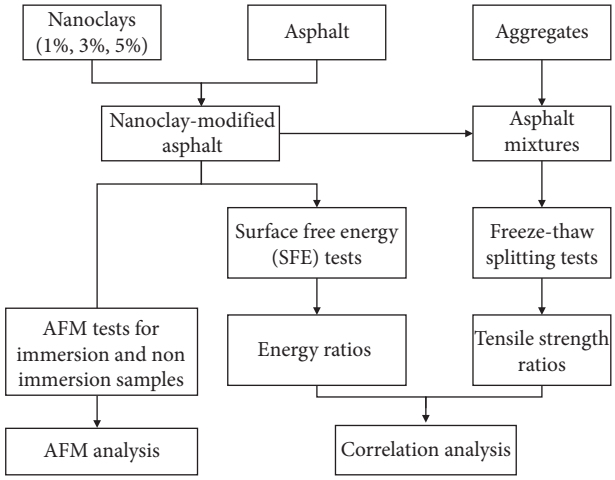

Figure 2: Flow chart for this study.

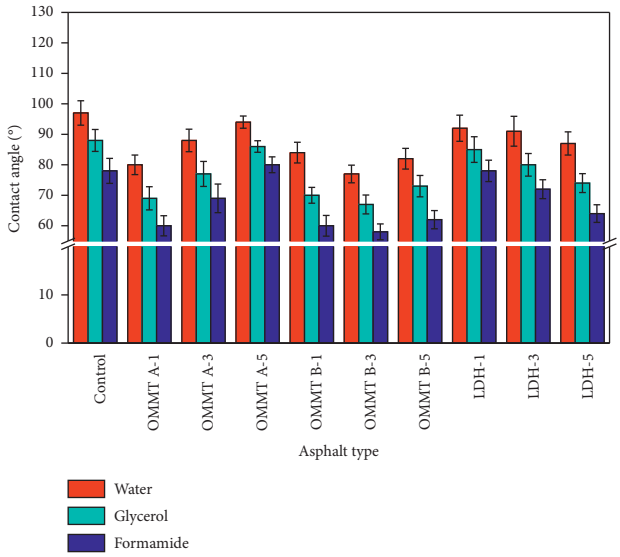

Figure 3: Average contact angles for the probe liquids.

significant reduction (about 49%) of the nonpolar components was observed in OMMT A-5, as was the most significant reduction (about 42%) of the total SFE.

When OMMT A was used to modify the asphalt, the binder modified with 1% OMMT A showed the highest SFE. As the dose of OMMT A was increased, the SFE of the modified asphalt was gradually reduced, although it remained greater than that of the control asphalt.

In the case of using OMMT B as a modifier, the effect of adding the nanoclay improved the SFE of the asphalt binders at additive amounts of 1% and 5% by weight of the base asphalt. When 3% of the OMMT B was added into the asphalt, the binder showed a reduced SFE, although this reduction was not significant.

Different trends were observed in the binders modified with LDH. The total SFE of LDH-1 was 35% lower than that of the control asphalt. However, as the amount of additive increased, the SFE of asphalt was gradually improved. When the dosage of the modifier reached 5%, there was no significant difference between the LDH-modified asphalt and the control asphalt considering the SFE.

3.1.3. Work of Adhesion. W_{ab} (the work of adhesion under dry conditions) and W_{abw} (the work of debonding in the presence of water) for the bitumen samples with different types of aggregates were calculated and are presented in Figures 6(a) and 6(b). Both the SBS-modified asphalt and nanoclay-modified asphalts were evaluated.

From Figure 6(a), it is shown that W_{ab} increased with the addition of all three types of nanoclays. As was shown in the study by Howson et al., a high W_{ab} indicates a high bond strength between the aggregate and asphalt under anhydrous conditions [51]. Therefore, the bond strength under anhydrous conditions was improved with the addition of the nanoclays. In terms of the aggregate types, although the W_{ab} values of the different aggregates showed similar increasing trends, the increases of limestone1 and limestone2 are more significant compared with basalt. In other words, according to this enhancement of W_{ab}, the effect of adding nanoclays to a system comprised of binders and limestone is more effective than that achieved for a system comprised of binders and basalt.

Among all of the asphalt binders, OMMT B-3 had the highest increase in W_{ab} values (from 34% for basalt to 76% for limestone1). In the case of the asphalts modified with OMMT A and LDH, OMMT A-1 showed higher W_{ab} values than OMMT A-3 and OMMT A-5, while LDH-5 had a higher W_{ab} than LDH-1 and LDH-3.

It can be seen that the absolute values of W_{abw} for the nanoclay-modified asphalts decreased for both limestone1 and limestone2. As a low absolute value of W_{abw} signifies a low potential for water damage [21], it could be said that the addition of nanoclays enhanced the moisture resistances of the systems composed of limestone and the asphalt binders. The reduction of this value was most significant in the case of OMMT B-3 (21% for both limestone1 and limestone2). The effects of the nanoclays on the systems composed of basalt and the binders are similar to those for the systems composed of limestone and the binders, with the exception of OMMT B-5 and LDH-1. In these two exceptional cases, the absolute values of W_{abw} showed a slight increase.

In brief, the addition of nanoclay can improve the water resistance of asphalt-aggregate systems, which is due to the molecular orientation changes of modified asphalt, the hydrophilicity decreases, and the adhesion between the asphalt-aggregate surface is strengthened.

As mentioned above, the energy ratio (ER) may be calculated using W_{ab} and W_{abw}. These indicators are discussed next.

3.1.4. Energy Ratio. The energy ratio (ER) is an index that quantifies the moisture damage potential [13]. A high ER value indicates that the system consisting of binders and aggregates has great resistance to moisture damage in the presence of water [5, 21]. The ER values of the different binder-aggregate systems are presented in Figure 7.

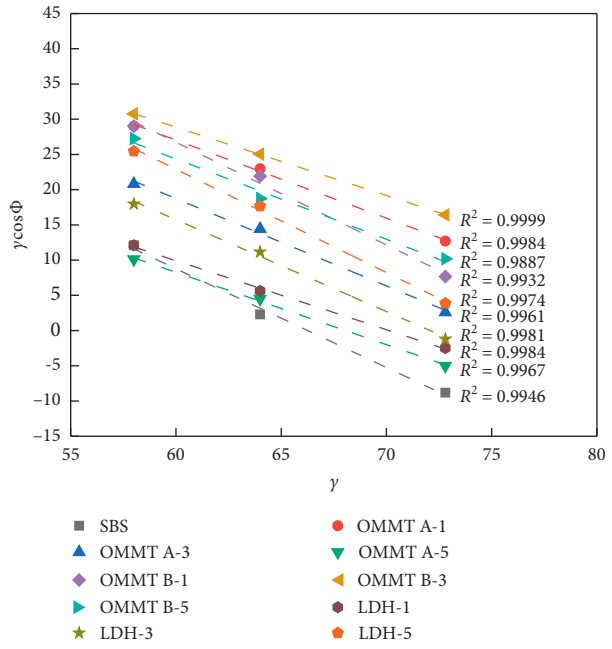

Figure 4: Plot of γ cosΦ versus γ.

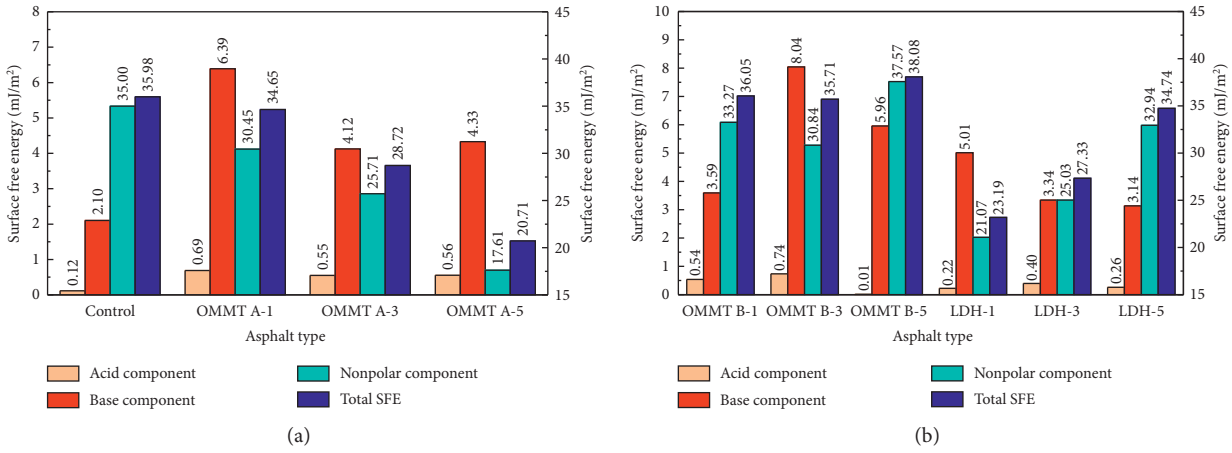

Figure 5: SFE components of the binders: (a) control and OMMT-A-modified asphalts; (b) OMMT-B- and LDH-modified asphalts.

As discussed previously, the addition of nanoclay markedly improved the W_{ab} of bitumen while reducing the absolute values of W_{abw} in most cases. As a result, the energy ratio (ER) parameter was improved significantly.

As shown in Figure 7, LDH can improve the ER of systems composed of asphalt binders and aggregates. In the limestone-binder systems, the ER did not change significantly when the dosage of the LDH increased from 1% to 3%. However, when the dosage of LDH was further increased, the ER values increased due to the rise of W_{ab}. In the case of the basalt-binder systems, the ER value gradually increased as the dosage of LDH was increased. When the dosage of LDH was increased to 5% by the weight of the bitumen, the improvement in the ER value was prominent (a 57% improvement for basalt).

A different trend was noticed when OMMT A was used as a modifier. Although the ERs for the OMMT-A-modified asphalts were all significantly higher than those of the control asphalt irrespective of the type of aggregate that was used, a different tendency from the LDH-modified asphalts was observed. More precisely, the ER values of the OMMT-A-modified asphalts decreased with increasing amounts of OMMT A due to the reduction of the work of adhesion under dry conditions.

The ER values of the systems composed of basalt- and OMMT-B-modified asphalt showed the same trend as the systems composed of basalt- and OMMT-A-modified asphalt. However, in the case of the limestone-binder systems, the ER increased when the dosage of OMMT B increased from 1% to 3%, and it was then reduced when the dosage

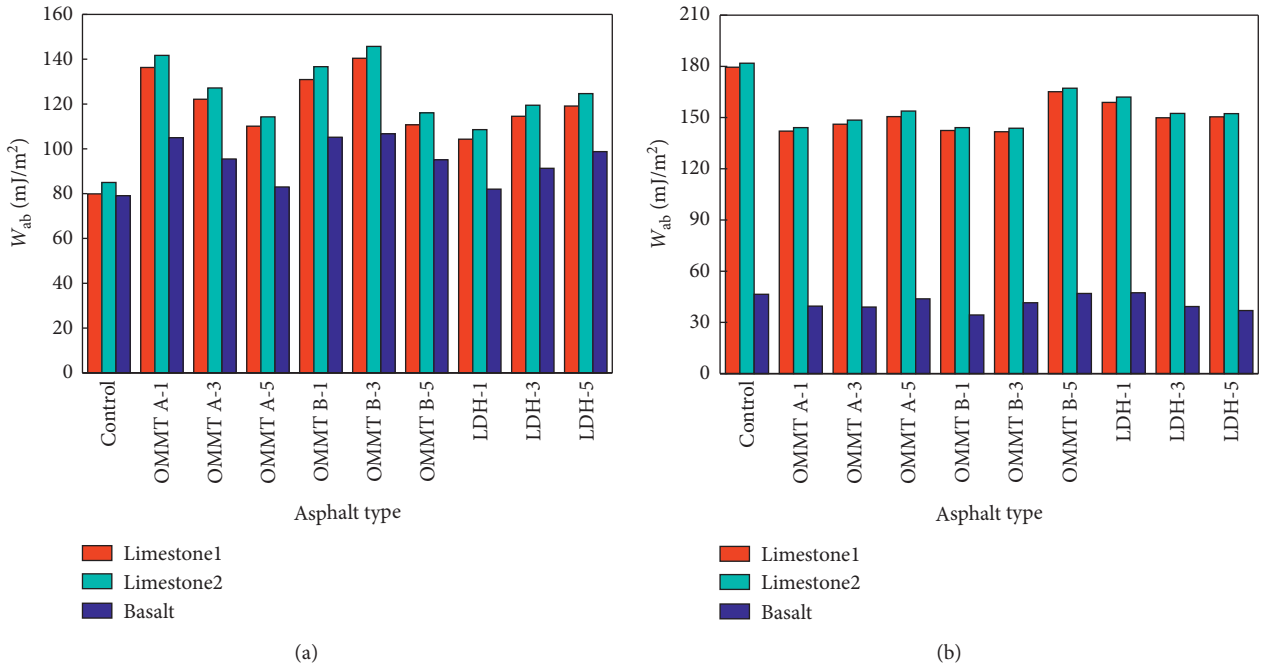

FIGURE 6: W_{ab} and W_{abw} of the bitumen with different types of limestone: (a) work of adhesion under dry conditions (W_{ab}) for the asphalt; (b) work of adhesion in the presence of water (W_{abw}) for the asphalt.

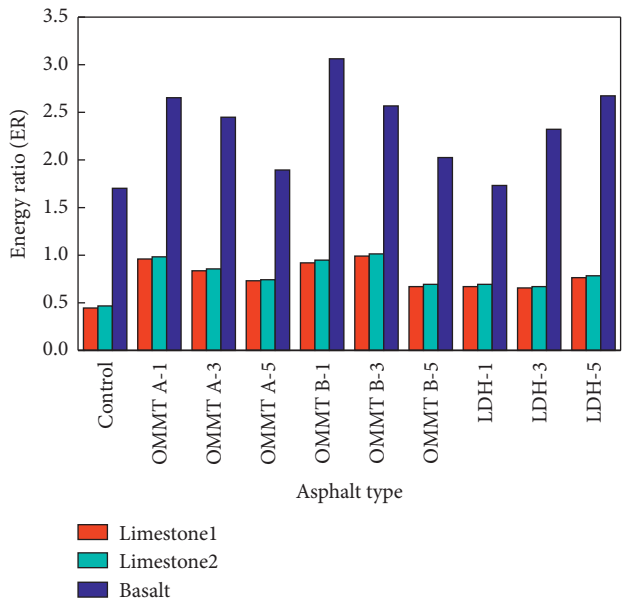

FIGURE 7: Energy ratios of bitumen with different types of limestone.

increased from 3% to 5%. This trend is consistent with the research of Omar et al. [5].

Among all of the nanoclay-modified asphalt binders considered in this article, OMMT B-3 showed the highest ER in conjunction with the limestones (limestone1 and limestone2). Meanwhile, OMMT A-1, OMMT B-1, and LDH-5 showed the highest ER values with basalt. Because a high ER value can be achieved with a relatively low dosage (1%), OMMT A and OMMT B have high potential for application in real-world engineering projects. Moreover, as shown in Figure 7, basalt demonstrated better compatibility with the modified binders than the limestones in terms of the ER.

3.2. Atomic Force Microscopy Analysis

3.2.1. Topographic Imaging. As mentioned above, AFM is a method used to study the performances of asphalt binders at a microscale [25, 38, 39]. In this study, the two asphalts with the considerable resistances to water damage as determined by the SFE testing, as well as the SBS-modified asphalt, were selected for AFM testing.

Atomic force microscopy was used to observe the microscale morphologies of the samples in the immersion and nonimmersion groups to determine the effects of water on the microstructures of asphalt. The effects of nanoclay on improving the resistance of asphalt to water damage were also examined.

The two-dimensional topography images of the SBS-modified asphalt binders, as well as the OMMT A-1 and LDH-5 asphalt samples, are shown in Figure 8 for both the nonimmersion and immersion groups. Every image in Figure 8 shows a $30 \times 30\,\mu$m region on the surfaces of the binders. The regions were selected at random.

Different colors in the images represent different heights. For instance, the white areas represent protrusions, while the black areas represent valleys. Bee structures, which consist of a combination of peaks and valleys, are easily observed in Figure 8.

The detailed three-dimensional images can be seen in Figure 9, which also indicates the relationship between the height and color in the color bar. From Figures 8 and 9, it can be observed that the bee-structures noted in the 2D images

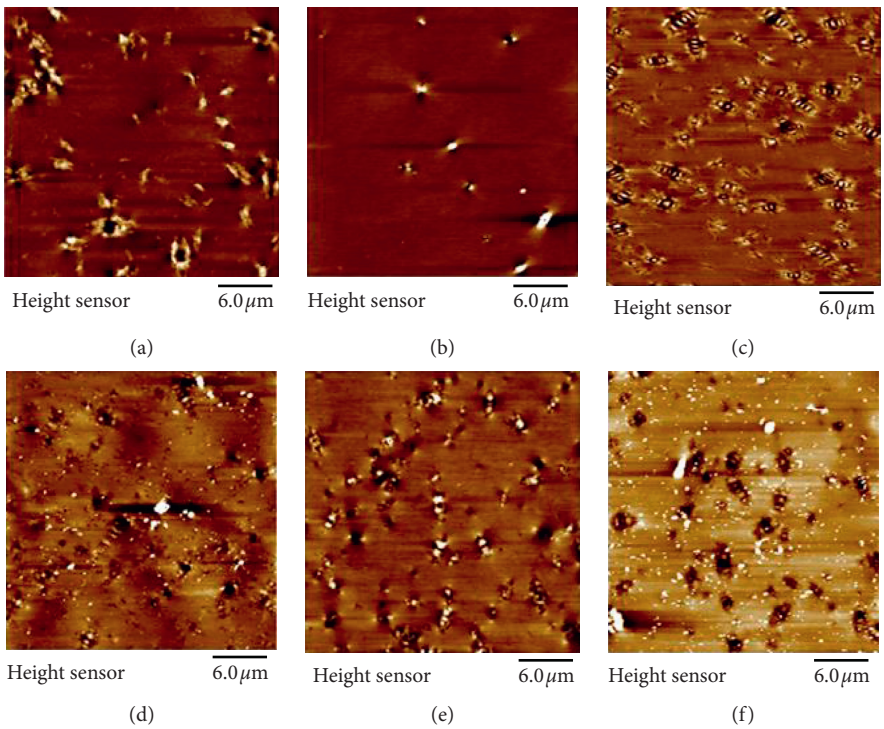

Figure 8: Two-dimensional topography images of the three asphalts: (a) SBS-modified asphalt; (b) SBS-modified asphalt after immersion; (c) OMMT A-1; (d) OMMT A-1 after immersion; (e) LDH-5; (f) LDH-5 after immersion.

consisted of bulges and pits, as shown in the 3D images. The appearance of the bee structure was attributed to the presence of asphaltenes by Li et al. and Yang et al. [52, 53]. Lu et al. and Yao et al. suggested that the wax content in bitumen is associated with the formation of the bee structure [54, 55]. Previous studies have suggested that the bee structure is associated with water damage to the asphalt [41,56]. More specifically, the exposure of the bitumen films to water led to the deformation of the microstructures. Under the influence of hydrostatic pressure and interfacial tension, the weak portions of the surface structures, such as the valleys in the bee structure and the interface between the periphase and the perpetua phase, will be deformed and damaged, resulting in the erosion of the microstructures and the reduction of the bee structures [41, 55, 56].

By comparing the images of the nonimmersion group samples in Figures 8(a), 8(c), and 8(e), it can be seen that the asphalt binders modified with nanoclays possess a larger amount of bee structures than the control asphalt. This phenomenon may be caused by the dipole-dipole interaction between the nanoclay and macromolecules such as resin and asphaltene [22, 57].

By comparing the surface morphologies of the three types of asphalt in the nonimmersion and immersion groups in Figure 8, it can be observed that the number of beestructures on the surface of the SBS-modified asphalt decreased after 24 h of immersion due to the exposure of the bitumen films to water. This variation caused by the effects of water contact is consistent with that found in studies by Yao et al. [55] and Vasconcelos et al. [56]. Additionally, it can be clearly seen from the three-dimensional image in Figure 9(b) that the microsurface structure of the SBS-modified asphalt tends to become flat after immersion.

The nanoclay-modified asphalt samples differed somewhat from the SBS-modified asphalt. After immersion in water, although the bee structure on the surface of the OMMT A-1 asphalt binder sample decreased, the residual amount of this surface topography was greater than that of the SBS-modified asphalt. In addition, pits and nanobumps were observed on the surface of the asphalt sample after immersion, a result similar to those obtained in studies by Tarefder and Arifuzzaman [58] and dos Santos et al. [41]. For LDH-modified asphalt, a decrease in the number of beestructures was observed after immersion between Figures 8(e) and 8(f). However, the areas of the individual bee structures were observed to increase. Moreover, the peaks and valleys that form this bee structure were more obvious in the three-dimensional structure after immersion. The pits and nanobumps were also observed in the case of the water-immersed LDH-5 sample.

In brief, considering the effects of water, a decrease in the number of bee structures was found on the surfaces of both the SBS-modified asphalt and nanoclay-modified asphalts. This occurred because the weak parts portions of the surface structures, such as the valleys in the bee structure and the interface between the periphase and the perpetua phase, are deformed and damaged due to hydrostatic pressure and interfacial tension [41,55,56]. However, the residual amount

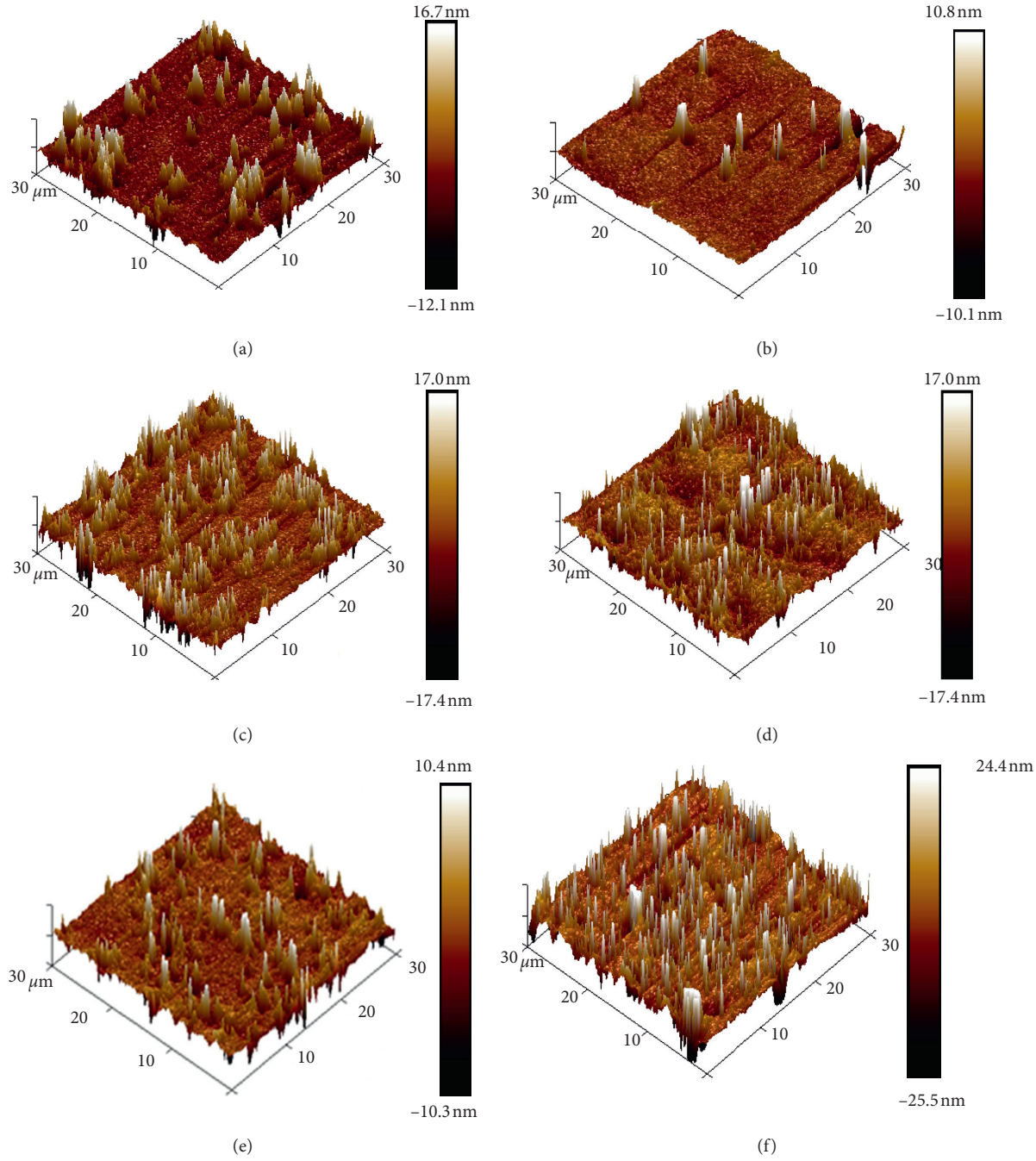

Figure 9: Three-dimensional height images of the three asphalts: (a) SBS-modified asphalt; (b) SBS-modified asphalt after immersion; (c) OMMT A-1; (d) OMMT A-1 after immersion; (e) LDH-1; (f) LDH-1 after immersion.

of bee structures was higher in the case of the nanoclay-modified asphalts compared to the SBS-modified asphalt. This may indicate that the addition of nanoclay makes the surface morphology of asphalt more resistant to water damage.

According to previous studies, nanoclays-modified asphalt prepared by the melt blending method usually formed exfoliated or semiexfoliated nanostructure, which could retard the infiltration and diffusion of moisture in asphalt [21,59,60]. This may explain why modified asphalt samples show better water stability in the process of soaking.

3.2.2. Roughness. Roughness is an index used to evaluate the undulation of the surface microstructures [31,61,62]. Considering the effects of water, there is no definite rule in the change in roughness that may occur as a result of water contact. The asphalt type, modifier type, aging effects, probe type, and other factors will all affect the changes in roughness that occur in the presence of water [31,39,62,63].

The roughness values were calculated using the NanoScope Analysis software from the topographic images provided by atomic force microscopy. The results are shown

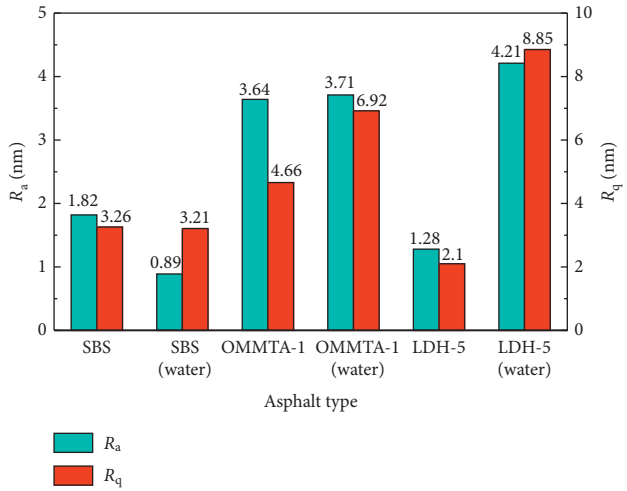

Figure 10: Roughness variation for the three types of asphalt before and after immersion.

in Figure 10, wherein R_a represents the mean height and R_q represents the mean variance of the height.

As can be seen from Figure 10, the roughness values of all three types of asphalt changed after water immersion. The immersion process occurred over 24 h at 25°C, followed by drying at the same temperature for 72 h.

In Figure 10, it is observed that the roughness values of the SBS-modified asphalt decreased, whereas those of the nanoclay-modified asphalts increased after undergoing immersion in water. This may be related to the pits and nanobumps previously observed in the 2D and 3D topographic images of the nanoclays-modified asphalts after immersion.

3.3. Freeze-Thaw Splitting Test. The freeze-thaw splitting test is a traditional method used to evaluate the water sensitivity of an asphalt mixture. Although this method cannot reveal the processes and mechanisms of water damage at the molecular or nanoscales, it can be used to verify the results of other tests, such as the SFE test, because it may correlate well with these other tests. The results of the freeze-thaw splitting tests are depicted in Figure 11.

By comparing the TSRs with the ERs of the systems of binders and basalt depicted in Figure 11, it can be easily observed that these two indicators exhibit similar trends when nanoclays are added to the asphalt and asphalt mixtures. These similar trends indicate the validity of the results obtained in the surface energy tests. The TSRs of the nanoclay-modified asphalts are higher than that of the SBS-modified asphalt, which also verifies the results of the AFM tests.

The linear correlation between the TSRs and ERs is depicted in Figure 12. The coefficient of determination (R^2) for this correlation is 0.6896. Although the coefficient of determination (R^2) is not very high, considering the complexity of the asphalt compositions and many other factors that may influence this relationship, this relationship can be considered to be good between these two indicators.

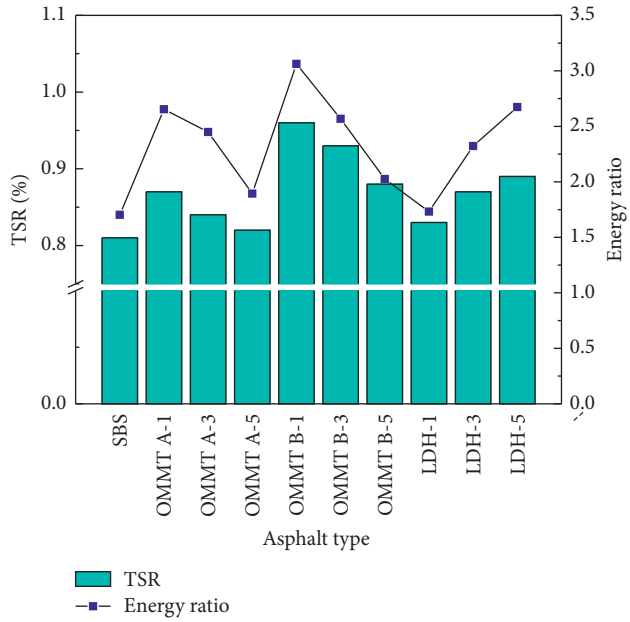

Figure 11: Tensile strength ratios (TSRs) obtained from freeze-thaw splitting tests and ERs of the systems of binders and basalt.

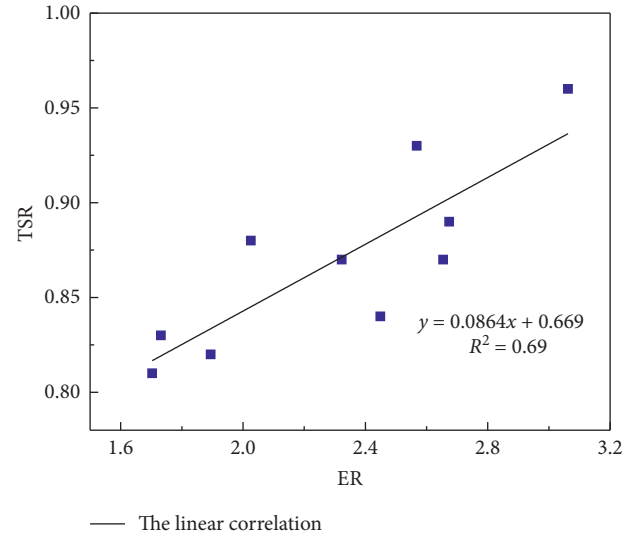

Figure 12: Relationship between TSR and ER values.

4. Conclusions

In this study, varied dosages of three types of nanoclays were used to modify SBS-modified asphalt binders. The resistance to moisture damage of the modified binders was evaluated through the SFE technique. AFM was used to determine the effects of water immersion on the microstructures of the asphalt and the effects of the nanoclays on the resistance of asphalt to water damage. Additionally, freeze-thaw splitting tests were used to verify the results obtained through the SFE and AFM tests. Based on the obtained results, the following conclusions may be drawn:

(1) Although general improvements can be clearly observed for the acidic and basic components of all modified binders, the total SFE values decreased when the asphalt was modified with the nanoclays. This reduction is mainly because of the decreased nonpolar components, which play a dominant role in the total SFE of these binders.

(2) The bond strength between the aggregate-binder systems under an anhydrous condition was enhanced with the addition of nanoclays. This enhancement was more significant for the limestones than basalt. Additionally, the work of debonding in the presence of water decreased in terms of the absolute value due to this modification.

(3) The addition of nanoclays improved the moisture resistances of the aggregate and modified binder systems. The degree of improvement differed depending on the types and dosages of nanoclay, as well as the type of aggregate. Moreover, in terms of the ER for binders with different aggregates, basalt demonstrated better compatibility with modified binders than limestones (for both limestone1 and limestone2).

(4) As a result of the hydrostatic pressure and interfacial tension from water immersion, the weak areas of the surface structures, such as the valleys in the bee structures and the interface between the periphase and the perpetua phase, became deformed and damaged. This process resulted in a decreased number of bee structures on the surfaces of both the SBS-modified asphalt and nanoclay-modified asphalts after immersion. However, the residual amount of the bee-structures was higher in the case of the nanoclay-modified asphalts than in the case of the SBS-modified asphalt. This may indicate that the addition of nanoclay makes the surface morphology of asphalt more resistant to water damage.

(5) In terms of roughness after immersion, the roughness of the SBS-modified asphalt decreased, whereas the roughness of the nanoclay-modified asphalts increased. This may be related to the pits and nanobumps observed on the surfaces of the nanoclay-modified asphalts after immersion.

(6) The results of the freeze-thaw splitting test correlate well with the results of the SFE and AFM tests, verifying the results obtained through these tests.

Data Availability

The data used to support the findings of this study are available from the corresponding author upon request.

Conflicts of Interest

The authors declare no conflicts of interest.

Authors' Contributions

Yinchuan Guo and Aiqin Shen conceptualized the study; Han Wang wrote the original draft; Xiaolong Yang and Peng Li wrote, reviewed, and edited the article.

Acknowledgments

This research was funded by the Natural Science Foundation for Youth of Shaanxi Provincial (Grant no. S2017-ZRJJ-QN-0944) and Science and Technology Project of Shaanxi Transportation and Transportation Department (Grant no. 10-26K).

References

[1] W. Wang, L. Wang, H. Xiong, and R. Luo, "A review and perspective for research on moisture damage in asphalt pavement induced by dynamic pore water pressure," *Construction and Building Materials*, vol. 204, pp. 631–642, 2019.

[2] D. Luo, A. Khater, Y. Yue et al., "The performance of asphalt mixtures modified with lignin fiber and glass fiber: a review," *Construction and Building Materials*, vol. 209, pp. 377–387, 2019.

[3] F. Saeed, M. Rahman, D. Chamberlain, and P. Collins, "Asphalt surface damage due to combined action of water and dynamic loading," *Construction and Building Materials*, vol. 196, pp. 530–538, 2019.

[4] A. Bhasin, E. Masad, D. Little, and R. Lytton, "Limits on adhesive bond energy for improved resistance of hot-mix asphalt to moisture damage," *Transportation Research Record: Journal of the Transportation Research Board*, vol. 1970, no. 1, pp. 2–13, 2006.

[5] H. A. Omar, N. I. M. Yusoff, H. Ceylan et al., "Determining the water damage resistance of nano-clay modified bitumens using the indirect tensile strength and surface free energy methods," *Construction and Building Materials*, vol. 167, pp. 391–402, 2018.

[6] M. R. Kakar, M. O. Hamzah, and J. Valentin, "A review on moisture damages of hot and warm mix asphalt and related investigations," *Journal of Cleaner Production*, vol. 99, pp. 39–58, 2015.

[7] A. A. Mamun and M. Arifuzzaman, "Nano-scale moisture damage evaluation of carbon nanotube-modified asphalt," *Construction and Building Materials*, vol. 193, pp. 268–275, 2018.

[8] R. Zhang, Z. You, H. Wang, M. Ye, Y. K. Yap, and C. Si, "The impact of bio-oil as rejuvenator for aged asphalt binder," *Construction and Building Materials*, vol. 196, pp. 134–143, 2019.

[9] S.-C. Huang, R. E. Robertson, J. F. Branthaver, and J. C. Petersen, "Impact of lime modification of asphalt and freeze–thaw cycling on the asphalt–aggregate interaction and moisture resistance to moisture damage," *Journal of Materials in Civil Engineering*, vol. 17, no. 6, 2005.

[10] Y. Jiao, Y. Zhang, L. Fu, M. Guo, and L. Zhang, "Influence of crumb rubber and tafpack super on performances of SBS modified porous asphalt mixtures," *Road Materials and Pavement Design*, vol. 20, no. 1, pp. S196–S216, 2019.

[11] F. Xiao, A. N. Amirkhanian, and S. N. Amirkhanian, "Long-term ageing influence on rheological characteristics of asphalt

binders containing carbon nanoparticles," *International Journal of Pavement Engineering*, vol. 12, no. 6, pp. 533–541, 2011.

[12] M. J. Khattak, A. Khattab, H. R. Rizvi, and P. Zhang, "The impact of carbon nano-fiber modification on asphalt binder rheology," *Construction and Building Materials*, vol. 30, pp. 257–264, 2012.

[13] H.-L. Zhang, M.-M. Su, S.-F. Zhao, Y.-P. Zhang, and Z.-P. Zhang, "High and low temperature properties of nanoparticles/polymer modified asphalt," *Construction and Building Materials*, vol. 114, pp. 323–332, 2016.

[14] H. Yao, Q. Dai, Z. You, M. Ye, and Y. K. Yap, "Rheological properties, low-temperature cracking resistance, and optical performance of exfoliated graphite nanoplatelets modified asphalt binder," *Construction and Building Materials*, vol. 113, pp. 988–996, 2016.

[15] G. Shafabakhsh, S. M. Mirabdolazimi, and M. Sadeghnejad, "Evaluation the effect of nano-TiO_2 on the rutting and fatigue behavior of asphalt mixtures," *Construction and Building Materials*, vol. 54, pp. 566–571, 2014.

[16] A. K. Das and D. Singh, "Effects of regular and nano sized hydrated lime fillers on fatigue and bond strength behavior of asphalt mastic," *Transportation Research Record: Journal of the Transportation Research Board*, vol. 2672, no. 28, pp. 31–41, 2018.

[17] R. Sezavar, G. Shafabakhsh, and S. M. Mirabdolazimi, "New model of moisture susceptibility of nano silica-modified asphalt concrete using GMDH algorithm," *Construction and Building Materials*, vol. 211, pp. 528–538, 2019.

[18] S. W. Goh, M. Akin, Z. You, and X. Shi, "Effect of deicing solutions on the tensile strength of micro- or nano-modified asphalt mixture," *Construction and Building Materials*, vol. 25, no. 1, pp. 195–200, 2011.

[19] P. K. Ashish, D. Singh, and S. Bohm, "Evaluation of rutting, fatigue and moisture damage performance of nanoclay modified asphalt binder," *Construction and Building Materials*, vol. 113, pp. 341–350, 2016.

[20] T. López-Montero, J. Crucho, L. Picado-Santos, and R. Miró, "Effect of nanomaterials on ageing and moisture damage using the indirect tensile strength test," *Construction and Building Materials*, vol. 168, pp. 31–40, 2018.

[21] Z. Hossain, M. Zaman, T. Hawa, and M. C. Saha, "Evaluation of moisture susceptibility of nanoclay-modified asphalt binders through the surface science approach," *Journal of Materials in Civil Engineering*, vol. 27, no. 10, 2015.

[22] L. Zhang and J. Cao, "Pyrolysis and its mechanism of organomontmorillonite (OMMT) influenced by different functional groups," *Journal of Thermal Analysis and Calorimetry*, vol. 137, no. 1, pp. 1–10, 2019.

[23] S. Sun, X. Li, G. Zheng, and L. Zhang, "Preparation and properties of nano-montmorillonite modified asphalt emulsion," *Materials Review*, vol. 29, no. 1, pp. 129–132, 2015.

[24] H. Zhang, J. Yu, and S. Wu, "Effect of montmorillonite organic modification on ultraviolet aging properties of SBS modified bitumen," *Construction and Building Materials*, vol. 27, no. 1, pp. 553–559, 2012.

[25] M. Jia, Z. Zhang, L. Wei et al., "Study on properties and mechanism of organic montmorillonite modified bitumens: view from the selection of organic reagents," *Construction and Building Materials*, vol. 217, pp. 331–342, 2019.

[26] Y. F. Huang, Z. G. Feng, H. L. Zhang, and J. Y. Yu, "Effect of layered double hydroxides (LDHs) on aging properties of bitumen," *Journal of Testing and Evaluation*, vol. 40, no. 5, pp. 734–739, 2012.

[27] L. Lupa, L. Cocheci, R. Pode, and I. Hulka, "Phenol adsorption using Aliquat 336 functionalized Zn-Al layered double hydroxide," *Separation and Purification Technology*, vol. 196, pp. 82–95, 2018.

[28] A. I. Alateyah, H. N. Dhakal, and Z. Y. Zhang, "Processing, properties, and applications of polymer nanocomposites based on layer silicates: a review," *Advances in Polymer Technology*, vol. 32, no. 4, 2013.

[29] D. X. Cheng, D. N. Little, R. L. Lytton, J. C. Holste, and A. Aapt, *Use of Surface Free Energy Properties of the Asphalt-Aggregate System to Predict Moisture Damage Potential*, American Association of Physics Teachers, College Park, MD, USA, 2002.

[30] S.-C. Huang, T. F. Turner, A. T. Pauli, F. P. Miknis, J. F. Branthaver, and R. E. Robertson, "Evaluation of different techniques for adhesive properties of asphalt-filler systems at interfacial region," in *Advances in Adhesives, Adhesion Science, and Testing*, D. Damico, Ed., pp. 114–128, ASTM International, West Conshohocken, PA, USA, 2005.

[31] K. Liu, L. Deng, J. Zheng, and K. Jiang, "Moisture induced damage of various asphalt binders," *Chinese Journal of Materials Research*, vol. 30, no. 10, pp. 773–780, 2016.

[32] M. H. Sadd, Q. Dai, V. Parameswaran, and A. Shukla, "Simulation of asphalt materials using finite element micromechanical model with damage mechanics," *Transportation Research Record: Journal of the Transportation Research Board*, vol. 1832, no. 1, pp. 86–95, 2003.

[33] G. H. Shafabakhsh, M. Faramarzi, and M. Sadeghnejad, "Use of surface free energy method to evaluate the moisture susceptibility of sulfur extended asphalts modified with anti-stripping agents," *Construction and Building Materials*, vol. 98, 2015.

[34] M. Gong, Z. Yao, Z. Xiong, J. Yang, and J. Hong, "Investigation on the influences of moisture on asphalts' micro properties by using atomic force microscopy and Fourier transform infrared spectroscopy," *Construction and Building Materials*, vol. 183, pp. 171–179, 2018.

[35] X. Yu, N. A. Burnham, R. B. Mallick, and M. Tao, "A systematic AFM-based method to measure adhesion differences between micron-sized domains in asphalt binders," *Fuel*, vol. 113, pp. 443–447, 2013.

[36] Y. Tan and M. Guo, "Using surface free energy method to study the cohesion and adhesion of asphalt mastic," *Construction and Building Materials*, vol. 47, pp. 254–260, 2013.

[37] D. X. Cheng, D. N. Little, R. L. Lytton, and J. C. Holste, *Surface Energy Measurement of Asphalt and Its Application to Predicting Fatigue and Healing in Asphalt Mixtures, Bituminous Binders 2002: Materials and Construction*, Transportation Research Board Natl Research Council, Washington, DC, USA, 2002.

[38] A. Obaid, M. D. Nazzal, L. Abu Qtaish et al., "Effect of RAP source on cracking resistance of asphalt mixtures with high RAP contents," *Journal of Materials in Civil Engineering*, vol. 31, no. 10, 2019.

[39] W. Zhang, L. Zou, Z. Jia, F. Wang, Y. Li, and P. Shi, "Effect of thermo-oxidative ageing on nano-morphology of bitumen," *Applied Sciences-Basel*, vol. 9, no. 15, 2019.

[40] A. Chen, G. Liu, Y. Zhao, J. Li, Y. Pan, and J. Zhou, "Research on the aging and rejuvenation mechanisms of asphalt using atomic force microscopy," *Construction and Building Materials*, vol. 167, pp. 177–184, 2018.

[41] S. dos Santos, M. N. Partl, and L. D. Poulikakos, "Newly observed effects of water on the microstructures of bitumen

surface," *Construction and Building Materials*, vol. 71, pp. 618–627, 2014.

[42] C. J. Van Oss, M. K. Chaudhury, and R. J. Good, "Interfacial Lifshitz-van der Waals and polar interactions in macroscopic systems," *Chemical Reviews*, vol. 88, no. 6, pp. 927–941, 1988.

[43] D. Singh and V. Mishra, "Different methods of selecting probe liquids to measure the surface free energy of asphalt binders," *Construction and Building Materials*, vol. 175, pp. 448–457, 2018.

[44] R. Ghabchi, D. Singh, and M. Zaman, "Evaluation of moisture susceptibility of asphalt mixes containing RAP and different types of aggregates and asphalt binders using the surface free energy method," *Construction and Building Materials*, vol. 73, pp. 479–489, 2014.

[45] A. Khodaii, V. Khalifeh, M. H. Dehnad, and G. H. Hamedi, "Evaluating the effect of Zycosoil on moisture damage of hot-mix asphalt using the surface energy method," *Journal of Materials in Civil Engineering*, vol. 26, no. 2, pp. 259–266, 2014.

[46] M. J. Qazizadeh, H. Farhad, A. Kavussi, and A. Sadeghi, "Evaluating the fatigue behavior of asphalt mixtures containing electric arc furnace and basic oxygen furnace slags using surface free energy estimation," *Journal of Cleaner Production*, vol. 188, pp. 355–361, 2018.

[47] X. Liu, X. Zou, X. Yang, and Z. Zhang, "Effect of material composition on antistripping performance of SBS modified asphalt mixture under dry and wet conditions," *Journal of Adhesion Science and Technology*, vol. 32, no. 14, pp. 1503–1516, 2018.

[48] W. Zhang, F. Wang, J. Shi, Z. Li, and X. Liang, "Experimental study on nano-parameters of styrene-butadiene-styrene block copolymer modified bitumen based on atomic force microscopy," *Polymers*, vol. 11, no. 6, 2019.

[49] H. Li, B. Li, Q. Wang, L. Li, and Y. Wang, "Adhesion of aged SBS modified asphalt binder containing warm mix additive based on surface free energy," *Materials Review*, vol. 31, no. 8, pp. 129–133, 2017.

[50] R. Wang, Z. Qi, R. Li, and J. Yue, "Investigation of the effect of aging on the thermodynamic parameters and the intrinsic healing capability of graphene oxide modified asphalt binders," *Construction and Building Materials*, vol. 230, 2020.

[51] J. Howson, E. Masad, A. Bhasin, D. Little, and R. Lytton, "Comprehensive analysis of surface free energy of asphalts and aggregates and the effects of changes in pH," *Construction and Building Materials*, vol. 25, no. 5, pp. 2554–2564, 2011.

[52] B. Li, J. Yang, Z. Chen, and H. Li, "Microstructure morphologies of asphalt binders using atomic force microscopy," *Journal of Wuhan University of Technology*, vol. 31, no. 6, pp. 1261–1266, 2016.

[53] J. Yang, M. Gong, X. Wang, X. Chen, X. Wang, and Z. Wang, "Observation and characterization of asphalt microstructure by atomic force microscopy," *Journal of Southeast University (English Edition)*, vol. 30, no. 3, pp. 353–357, 2014.

[54] X. Lu, M. Langton, P. Olofsson, and P. Redelius, "Wax morphology in bitumen," *Journal of Materials Science*, vol. 40, no. 8, 2005.

[55] Z. Yao, H. Zhu, M. Gong, J. Yang, G. Xu, and Y. Zhong, "Characterization of asphalt materials' moisture susceptibility using multiple methods," *Construction and Building Materials*, vol. 155, pp. 286–295, 2017.

[56] K. L. Vasconcelos, A. Bhasin, and D. N. Little, "History dependence of water diffusion in asphalt binders," *International Journal of Pavement Engineering*, vol. 12, no. 5, pp. 497–506, 2011.

[57] L. Sun, X. Xin, H. Wang, and W. Gu, "Microscopic mechanism of modified asphalt by multi-dimensional and multi-scale nanomaterial," *Journal of the Chinese Ceramic Society*, vol. 40, no. 10, pp. 1437–1447, 2012.

[58] R. Tarefder and M. Arifuzzaman, *Moisture Damage Study of Plastomeric Polymer Modified Asphalt Binder Using Functionalized AFM Tips*, International Institute of Informatics and Systemics, Orlando, FL, USA, 2010.

[59] H. Zhang, J. Yu, and S. Wu, "Effect of montmorillonite organic modification on ultraviolet aging properties of SBS modified bitumen," *Construction and Building Materials*, vol. 27, no. 1, pp. 553–559, 2012.

[60] S. A. Bagshaw, T. Kemmitt, M. Waterland, and S. Brooke, "Effect of blending conditions on nano-clay bitumen nanocomposite properties," *Road Materials and Pavement Design*, vol. 20, no. 8, pp. 1735–1756, 2019.

[61] X. Cai, J. Y. Zhang, M. H. Gong, J. Yang, and X. H. Chen, "Investigation of aging behavior of biorejuvenated asphalt with chemical and micromechanical methods," *Journal of Testing and Evaluation*, vol. 47, no. 5, pp. 3605–3621, 2019.

[62] Q. Zhang and Z. Huang, "Investigation of the microcharacteristics of asphalt mastics under dry-wet and freeze-thaw cycles in a coastal salt environment," *Materials*, vol. 12, no. 16, 2019.

[63] H. H. Kim, M. Mazumder, and S.-J. Lee, "Micromorphology and rheology of warm binders depending on aging," *Journal of Materials in Civil Engineering*, vol. 29, no. 11, 2017.